Paleoseismological evidence of early-late Holocene surface faulting along the northeastern Himalayan front at the western flank of eastern syntaxis, India.

by R.Jayangondaperumal[1,2], Steven G.Wesnousky[2], B.K.Chaudhari[1]

[1,2]Corresponding author:

Wadia Institute of Himalayan Geology
Dehradun-248001, India

[2]Center for Neotectonic Studies
University of Nevada, Reno
Mail Stop 169
Reno, NV 89557

Email: ramperu@rediffmail.com

Abstract

We present here the results of a paleoseismic investigation at Marbang Korong Creek within the meizoseismal area of the 1950 Assam earthquake along the northeast Himalayan Frontal Thrust (HFT) of India. Structural, stratigraphic, and growth-stratigraphy relations observed in a trench excavated across a young scarp in alluvium at the mouth of the Creek records the occurrence of at least two Holocene earthquakes. Radiocarbon dating shows the penultimate and most recent events occurred post 8163 BC (Early Holocene) and Post 66 AD., respectively. The most recent event deformation could be related to either the 1100 AD earthquake event which has been reported previously at sites to the west or the more recent the 1950 Assam earthquake.

Key words: Holocene surface faulting, earthquake scarp, paleoseismology, growth stratigraphy, the 1100 AD and the 1950 AD Assam earthquake,

Introduction

The rate of convergence between the Indian and Eurasia plates is about 50 mm/year (Fig.1, DeMets et al., 1994; Banerjee and Bürgmann, 2002; Bilham et al., 1997; Patriat and Achache, 1984; Larson et al., 1999; Paul et al., 2001; Berger et al., 2004). Between 10 and 20 mm/yr of the convergence is accommodated by thrusting along the Himalayan Frontal Thrust (HFT) and the remainder by deformation further inland and to the north (Nakata et al., 1998; Nakata, 1989; Yeats et al., 1992; Wesnousky et al., 1999; Lavé and Avouac, 2000; Kumar et al., 2001; Mugnier et al., 2004; Lavé et al., 2005; Kumar et al., 2006; Malik and Nakata, 2003; Malik et al., 2008; Kumar et al., 2010). The HFT extends ~2000 km, from near Pakistan in the west to Pasighat in the east. There have now been a number of paleoseismic investigations that have placed limits on the size and age of past earthquake displacements along the HFT (Kumar et al., 2001; Kumar et al., 2006; Lave et al., 2005 and Fig. 1). Here we present the results of a trenching investigation to place limits on the past occurrence of large earthquakes along the HFT at the mouth of Marbang Korong Creek near Pasighat in Arunchal Pradesh. It is the easternmost of such studies that have thus far been conducted along the HFT. In this paper, we initially place the study site in regional context, then describe the geomorphic characteristics of the study site, and follow with

a description and interpretation of trench exposure. Finally, the results are placed in context of prior paleoseismic studies to the west of the study site.

Regional Tectonic Framework and Geomorphic Characteristics of Study Site

The study site is located within the meizoseismal zone of the 1950, Mw 8.4 Assam earthquake (Fig. 1, Poddar, 1950, Ambraseys, and Douglas, 2004). The 1950 earthquake occurred near the eastern syntaxis of the Himalayan front where the major thrusts and rock units of the Himalaya sharply change trend from northeast to southeast (Fig. 2). The trench is excavated across a strand of the HFT at the mouth of Marbang Korong creek. The fault trace, trench location, and major Quaternary surfaces in the vicinity of the trench are shown on a topographic map in Figure 3. Displacement on the HFT has produced an 8 m scarp in young alluvium across the mouth of Marbang Korong Creek (Fig. 3). Longer term displacement along the HFT has truncated and progressively offset two terrace surfaces along the creek. The lower and higher terrace surfaces sits about 8 meters and ~60 m above stream grade and are labeled LS and HS in Figure 3, respectively. The higher terrace surface is composed of sub angular to sub-rounded boulder to gravel with sand matrix, poorly sorted and inter-bedded sand layers of few cm to 0.5m thick, usually orange-red to orange to yellow color due to oxidations associated with weathering. The lower terrace surface (LS) is made of rounded pebble to boulder gravel in a silty sand matrix derived from the high Himalaya. The present day catchment of the Marbang Korong creek is confined to the Sub Himalaya (Fig. 3). In the lower terrace, the rounded to sub rounded large cobble and boulders are similar in composition, size and shape to those present in the adjoining Miku Korong and Remi rivers, suggesting that the lower terrace gravel originated in the higher Himalaya and Marbang Korong creek was once part of the Remi river system.

Trench Observations

A photo of the scarp trenched is shown in Figure 3. The areal and depth extent of the excavation are shown with respect to topography in Figure 4. The trench exposure was 26 m in length and ~5 m in depth (Fig.

5). A log of the trench exposure is shown in Figure 5, and a photo-mosaic of the exposure is provided in the electronic supplement. The oldest beds (unit 1) in the exposure are highly fractured Siwalik bedrock exposed in the lowest northern portion of the exposure. The Siwalik beds are overlain by Unit 2, a package of rounded to sub-rounded cobble, pebble and gravel, unconsolidated, matrix supported with distinct sand lenses and fabric that shows the deposits to bend and dip to 16° to the southeast. Both units 1 and 2 are broken by faults that dip steeply to the northwest. The bounding strands show normal displacement and form a small graben like structure. The gravel of unit 2 is overlain unconformably by two packages of horizontal to near horizontal bedded fine sand that are labeled unit 3 and 4 on the trench log (Fig. 5). The lowermost of the two units (unit 3) dips at about 10° to the southeast and is unconformably overlain by the horizontal beds of unit 4.

Trench Interpretation

The dipping beds of unit 2 are interpreted to represent the dip panel of a fold related to displacement on an underlying fault that does not reach the surface and fault displacement is recorded by warping of shallow sediments to form the observed scarp. In this regard, the normal faults observed in the trench are interpreted to be secondary in nature and the result of bending of beds near the scarp crest. The fine sands of units 3 and 4 are interpreted to be sediments that accumulate as flat lying beds along the scarp from periodic flooding of adjacent creeks and rivers. The tilting of unit 3 is thus interpreted to be the result of warping associated with one or more earthquakes subsequent to the deposition of unit 2 and prior to deposition of unit 4 beds which are currently flat lying. A schematic illustration of the geometry and process is provided in Figure 6.

Detrital charcoal samples P4 and P6 taken from deformed unit 2 (Fig. 5 and Table I) give calibrated ages of 9418-9114 BC and cal 8659-8163 BC, respectively. From these dates it is interpreted that one or more earthquakes created the observed scarp and dip panel subsequent to cal 8163 BC. An additional suite of 7 detrital charcoal samples was collected from units 3 and 4. A number of the ages do not follow observed stratigraphic order indicating that some of the charcoal is likely reworked from older units. In this regard, one may only infer that the ages of units 3 and 4 are equal to or younger than the youngest radiocarbon sample

extracted from the units. The youngest sample in the tilted beds of Unit 3 is P11 = cal 60 BC- 66 AD, from which we infer that the tilting of these beds is the result of an earthquake that occurred subsequent to cal 60 BC.

Discussion and Conclusions

Our observations indicate that at least one large scarp forming event occurred along the HFT at this site subsequent to 8163 BC and that at least one more earthquake contributed to formation of the scarp after 60 BC. Though chronological constraints on the timing of the displacements are poor, the study documents that large surface ruptures occur and extend to the eastern limits of the HFT. Like trenches that have previously been excavated along the HFT to the west (Kumar et al., 2010), the scarp at this site is principally due to warping and folding of surficial deposits rather than simple fault displacement. Finally, it is possible that all or part of the tilting of sediments that occurred post 60 B.C. is the result of either the ~1100 AD earthquake that has been documented further to the west (Kumar et al., 2010; Yule et al., 2006; Uppreti et al., 2000; Nakata et al., 1998; Lave et al., 2005) or the historical 1950 Assam earthquake (Poddar, 1950, Ambraseys, and Douglas, 2004).

Acknowledgements

This work was conducted under National Science Foundation (NSF) grant EAR-0609556 with the support of the NSF Tectonics and the Africa, Near East and South Asia Program in the office of International Science and Engineering Programs and a grant to R. Jayangondaperumal from the Wadia Institute of Himalayan Geology. This paper was written while RJ was in the Center for Neotectonic Studies, University of Nevada, Reno, under the BOYSCAST fellowship program of DST, Govt. of India. We thank Miglung villagers and School master for their kindness to support our trenching work and providing permission to trench. Center for Neotectonic contribution #

References

Ambraseys, N., and J. Douglas (2004). Magnitude calibration of north Indian earthquakes, *Geophys. J. Int.* **159,** 165-206.

Banerjee, P., and R. Bürgmann (2002). Convergence across the northwest Himalaya from GPS measurements, *Geophysical Research Letter* **29(13),** 30-1 – 30-4.

Berger, A., F. Jouanne, R. Hassani, and J. L. Mugnier (2004). Modelling the spatial distribution of present-day deformation in Nepal: how cylindrical is the Main Himalayan Thrust in Nepal?, *Geophysical Journal International* **156 (1),** 94–114.

Bilham, R., K. Larson, J. Freymueller, and Others (1997). GPS measurements of present-day convergence across the Nepal Himalaya, *Nature*, **386,** 61-64.

Choudhuri, B.K., N.S. Gururajan, and R.K. Bikramaditya Singh (2009). Geology and structural evolution of the eastern Himalayan Syntaxis, *Himalayan Geology* **30 (1),** 17-34.

DeMets, C., R. G. Gordon, D. F. Argus, and S. Stein (1994). Effect of recent revisions to the geomagnetic reversal time scale on estimates of current plate motions, Geophys. *Res. Lett.* **21(20),** 2191–2194, doi:10.1029/94GL02118.

Kumar, S., S. G. Wesnousky, T.K. Rockwell, D. Ragona, V.C. Thakur, and G.G. Seitz (2001).Earthquake recurrence and rupture dynamics of Himalayan frontal thrust, *Science* **294,** 2328–2331.

Kumar, S., S.G. Wesnousky, T.K. Rockwell, R.W. Briggs, V.C. Thakur, and R. Jayangondaperumal (2006). Paleoseismic evidence of great surface rupture earthquakes along the Indian Himalaya, *Journal of Geophysical Research* **111,** B03304, doi:10.1029/2004JB003309.

Kumar, S., S.G. Wesnousky, R.Jayangondaperumal, T. Nakata, Y. Kumahara, and V. Singh (2010, in press) Paleoseismological evidence of surface faulting along the northeastern Himalayan front, India: Timing, Size, and Spatial Extent of Great Earthquakes, *Journal of Geophysical Research (B)* 2009JB006789

Larson, K., R. Bürgmann, R. Bilham, and J.T. Freymueller (1999). Kinematics of the India-Eurasia collision zone from GPS measurements, *J. Geophys. Res.* **104,** 1077-1093.

Lavé, J., and J. P. Avouac (2000). Active folding of fluvial terraces across the Siwaliks Hills, Himalayas of central Nepal, *J. Geophys. Res.* ***105*****(B3),** 5735-5770.

Lave´, J., D. Yule, S. Sapkota, K. Basant, C. Madden, M. Attal, and R. Pandey (2005). Evidence for a Great Medieval Earthquake (1100 A.D.) in the Central Himalayas, Nepal, *Science* **307,** 1302-1305.

Malik, J. N., and T. Nakata (2003). Active faults and related Late Quaternary deformation along the northwestern Himalayan Frontal Zone, India, *Ann. Geophys.* ***46*****,** 917-936.

Malik, J. N., T. Nakata, G. Philip, N. Suresh, and N.S. Virdi (2008). Active fault and paleoseismic investigation: evidence of historic earthquake along Chandigarh Fault in the frontal Himalayan zone, NW India, *Journal of Himalayan Geology* **29(2),** 109-117.

Mugnier, J. L., P. Huyghe, P. Leturm, and F. Jouanne (2004). Episodicity and rates of thrust sheet motion in the Himalayas (western Nepal), in Thrust tectonics and hydrocarbon systems, K. R. McClay (Editor), *AAPG Memoir* **82,** 91– 114.

Nakata, T. (1989). Special Paper 232, Active faults of the Himalaya of India and Nepal, in Tectonics of the Western Himalayas, L. L. Malinconico Jr. and R. J. Lillie (Editors), Geological Society of America, Boulder, Colorado, 243–264.

Nakata, T., et al. (1998), First successful paleoseismic trench study on active faults in the Himalaya (abstract), Eos Trans. AGU, 79(45), Fall Meet. Suppl., F615.

Patriat, P., and J. Achache (1984). India-Eurasia collision chronology has implications for crustal shortening and driving mechanism of plates, *Nature* **311,** 615-621.

Poddar, M.C. (1950). The Assam earthquake of 15th August 1950, *Indian Miner.* **4,** 167–176.

Reimer P.J, M.G.L. Baillie, E. Bard, A. Bayliss, J.W. Beck, P.G. Blackwell, C. Bronk Ramsey, C.E. Buck, G.S. Burr, R.L. Edwards, M. Friedrich, P.M. Grootes, T.P. Guilderson, I. Hajdas, T.J. Heaton, A.G.Hogg, K.A. Hughen, K.F. Kaiser, B. Kromer, F.G. McCormac, S.W. Manning, R.W. Reimer, D.A. Richards, J.R. Southon, S. Talamo, C.S.M. Turney, J. van der Plicht, and C.E. Weyhenmeyer (2009). IntCal09 and Marine09 radiocarbon age calibration curves, 0–50,000 years cal BP, *Radiocarbon* **51(4),** 1111–50

Seeber, L., and J. Armbruster (1981). Great detachment earthquakes along the Himalayan Arc and long-term forecasting, in Earthquake Prediction in an International Review, Maurice Ewing Ser., vol. 4 D. W. Simpson and P. G. Richards (Editors), pp. 259–277, AGU, Washington, D. C.

Stuiver, M., and P. J. Reimer (1993). Extended (super 14) C data base and revised CALIB 3.0 (super 14) C age calibration program, *Radiocarbon* ***35*****(1),** 215-230.

Upreti, B. N. and others (2000). The latest active faulting in Southeast Nepal, paper presented at Proceedings Active Fault Research for the New Millenium - Hokudan International Symposium and School on Active Faulting, Awaji Island, Hyogo Japan.

Wesnousky, S. G., S. Kumar, R. Mohindra, and V.C. Thakur (1999). Uplift and convergence along the Himalayan Frontal Thrust, *Tectonics* **18(6),** 967-976.

Yeats, R. S., T. Nakata, A. Farah, M. Fort, M. A. Mirza, M.R. Pandey, and R.S.Stein (1992).The Himalayan frontal fault system, *Annale Tectonicae* **6 (suppl.),** 85-98.

Yule, D., et al. (2006), Possible evidence for surface rupture of the Main Frontal Thrust during the great 1505 Himalayan Earthquake, Far-Western Nepal, paper presented at AGU, Fall Meeting, American Geophysical Union.

Additional Author Information

R.Jayangondaperumal[12], Steven G. Wesnousky[2], and B.K.Chaudhari[1]

[1]Wadia Institute of Himalayan Geology
Dehradun-248001, India

[2]Center for Neotectonic Studies
University of Nevada, Reno
Mail Stop 169
Reno, NV 89557

Tables

Table 1

Calibrated ^{14}C AMS ages of Marbang Korong Trench.

Electronic Supplement 1

A photomosaic of the Marbang Korong Creek Trench, Arunachal Pradesh, India.

Figure Captions

Figure 1

(Top) A simplified map of the Himalayan arc showing distributions of active faults in India, Nepal and Tibet together with historical earthquakes ruptures extent (after Kumar et al., 2006). The inferred rupture extent of major historical earthquakes along the Himalayan arc are: the 1505 central Himalayan earthquake (M*w* ~8.2), the 1555 Kashmir earthquake (M*w* ~7.6), the 1803 Kumaon-Garhwal earthquake (M*w* ~7.5), the 1833 Nepal earthquake (M*w* ~7.3), the 1905 Kangra earthquake (M*w* ~7.8), the 1934 Bihar-Nepal earthquake (M*w* ~8.1), the 1950 Assam earthquake (M*w* ~8.4), and the 2005 Kashmir earthquake (Mw 7.6) are shown as solid shaded irregular polygons with year. The speculative ruptures are shown as dotted polygons. Previous trench locations and associated ruptures event are shown in the map as black solid line with author's names. A thick box corresponds to present study site and location of Figure 2.

Bottom) A simplified N-S structural cross section across the Central Nepal Himalaya showing major faults and longitudinal divisions of Himalaya. Location of cross section is shown on top map as a thick line with bars at end. Note: Major thrust faults sole into a major crustal décollement is known as Main Himalayan Thrust (MHT). Concentration of instrumental seismicity/earthquakes along MHT is shown as solid circles (adapted from Seeber and Armbruster, 1981). STD, South Tibet Detachment; MCT, Main Central Thrust; MBT, Main Boundary Thrust; HFT, Himalayan Frontal Thrust.

Figure 2

Map of the eastern syntaxis of north-eastern Indian Himalaya showing major faults with subdivisions of Himalaya together with location of a trench site marked as a thick arrow (modified after Choudhuri et al. (2009). The trench is located across the Himalayan Frontal Thrust (HFT) which marks the contact between the Siwalik rocks of the Sub Himalaya to the north and the Quaternary sediments of the Brahmaputra floodplain to the south. ITSZ, Indus-Tsangpo Suture zone STD, South Tibet Detachment; MCT, Main Central Thrust; MBT, Main Boundary Thrust; HFT, Himalayan Frontal Thrust.

Figure 3

a) Location of Marbang Creek trench site on Survey of India (SOI) 20 m contour interval topo-sheet. A thick line with circles at ends across the scarp is the location of trench excavated. The HFT here cuts and has progressively uplifted a higher (HS) and lower (LS) terrace surfaces. The trench is excavated across the scarp that bounds the LS surface. (b) Photo showing escarpment of HFT and the higher (HS) and lower (LS) terrace surfaces with Siwaliks in background. c) Trench site is on the scarp that cuts lower terrace surface. Car is for a scale.

Figure 4

a) Profile across the scarp on which trench was excavated surface is shown in Figure 3a as line with circles at ends based on survey using Leica Total station. The length and depth of trench in relation to the scarp profile is shaded. The location of secondary faults are shown as thick solid lines within the shaded area and numbers 1 to 4 correspond to units observed in the trench exposure.

Figure 5

A log of eastern wall of Marbang Korong trench. Numbers in white solid circles denote the major stratigraphic units observed in the trench. Secondary bending faults are marked as F1 to F3. Small stars connecting solid line with alpha numeric show location of sample, sample number and calibrated ^{14}C AMS ages for corresponding

samples respectively. Horizontal and vertical scales are same. See electronic supplement 1 for photo mosaic of the trench exposure.

Figure 6

A schematic cartoon illustrating possible stage wise development of bending of hanging wall sediments, secondary normal faults, and tilting of growth stratigraphy observed in the trench. Decreasing arrows depict hypothesized decrease in slip on fault surface as it reaches near surface. Numbers denote the major stratigraphic units observed in the trench.

Table 1

Lab code CAMS #	Material used	Sample number	Unit	$\delta^{13}C$	Un calibrated ages	95.4 % (2σ) cal age ranges in AD/BC*	Relative area under distributions
146088	Charcoal	P4	2	-25	9140±130	cal BC 8711 - 8664	0.019435
						cal BC 8659 - 8163	0.895289
						cal BC 8147 - 7967	0.085276
146089	Charcoal	P6	2	-25	9770±160	cal BC 9803 - 8732	1.0
146090	Charcoal	P10	4	-25	1980±35	cal BC 51- AD 86	0.987675
						cal AD 107-AD 118	0.012325
146091	Charcoal	P19	4	-25	3280±360	cal BC 2575-758	0.998579
						cal BC 683-670	0.001421
146153	Charcoal	P3	3	-25	2615±30	cal BC 828-769	1.0
146719	Charcoal	P2	3	-25	2440±30	cal BC 753-685	0.228865
						cal BC 668-632	0.090802
						cal BC 625-611	0.020584
						cal BC 597-406	0.659748
146720	Charcoal	P18	4	-25	2440±30	cal BC 751-686	0.233329
						cal BC 667-637	0.080219
						cal BC 622-614	0.009744
						cal BC 595-406	0.676707
146721	Charcoal	P11	3	-25	2010±30	cal BC 91-69	0.042806
						cal BC 60- AD 66	0.957194
146722	Charcoal	P20	4	-25	2225±30	cal BC 384-338	0.228292
						cal BC 330-203	0.771708

*Calib Rev 6.0.1 (http://calib.qub.ac.uk/calib/)

*Calibration Data set: intcal09 (Reimer et al., 2009). IntCal09 and Marine09 radiocarbon age calibration curves, 0–50,000 years cal BP. Calibration curve: (Northern Hemisphere terrestrial sample)

Figure1

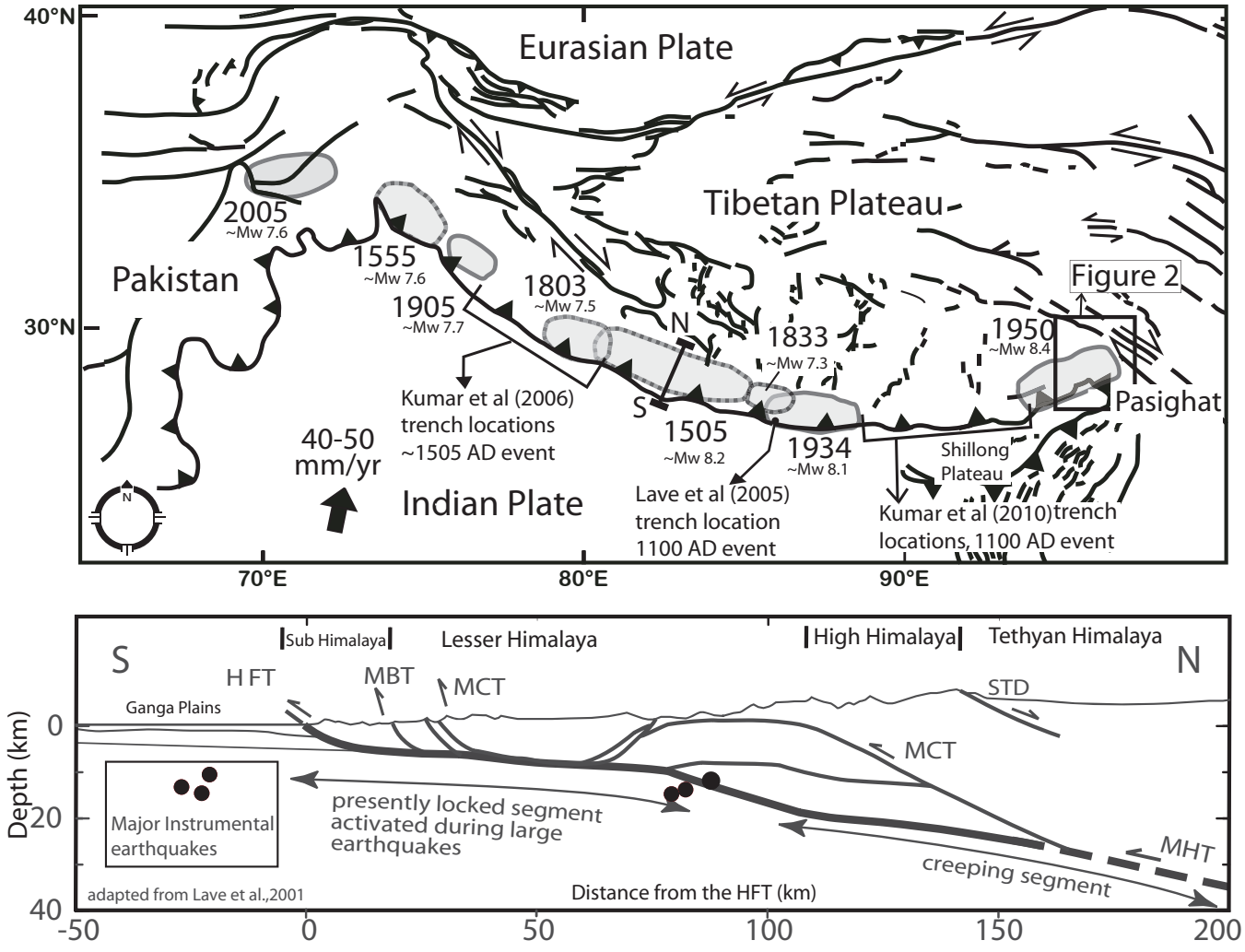

Figure 1

Figure2

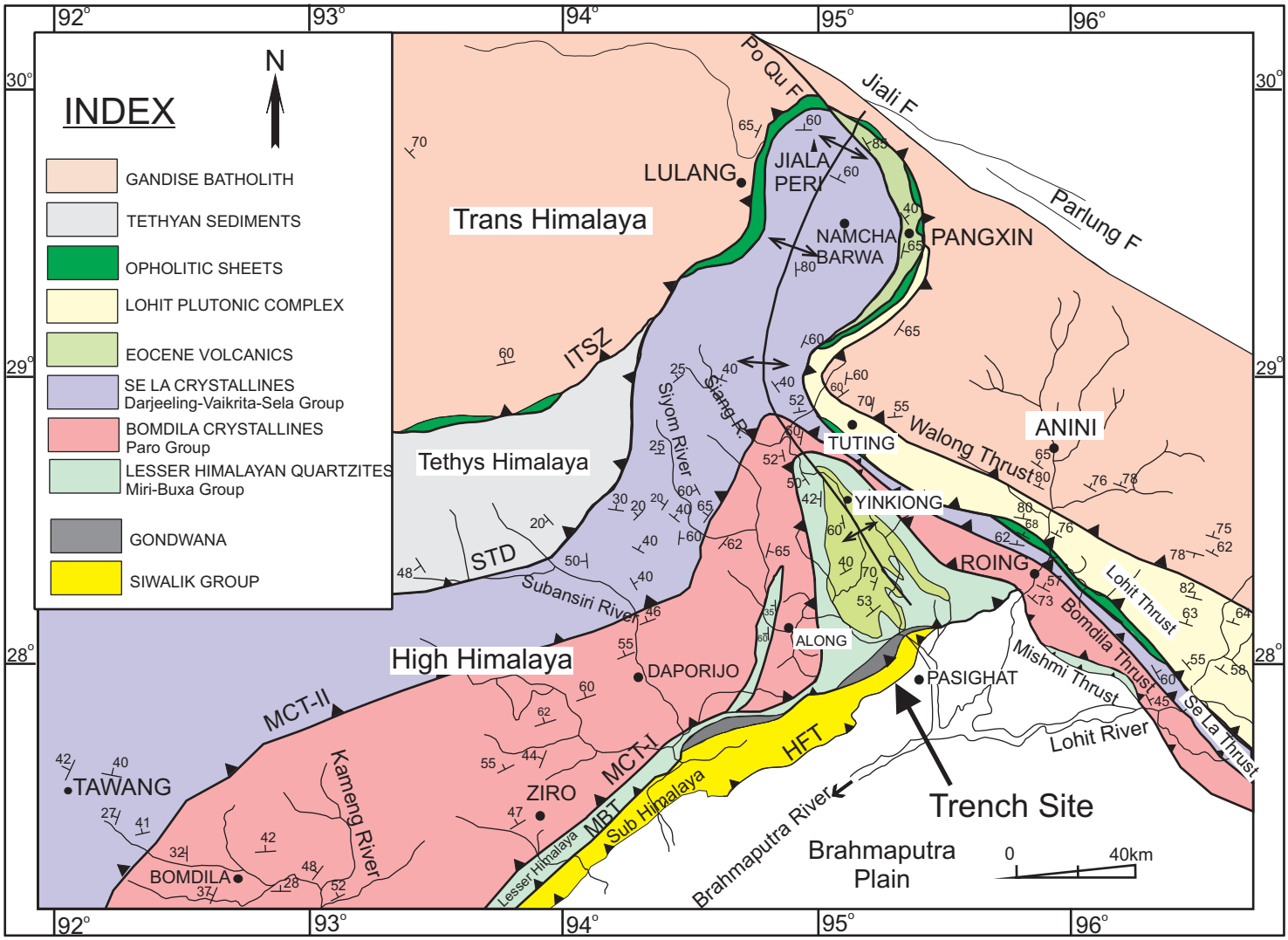

Figure 2

Figure3

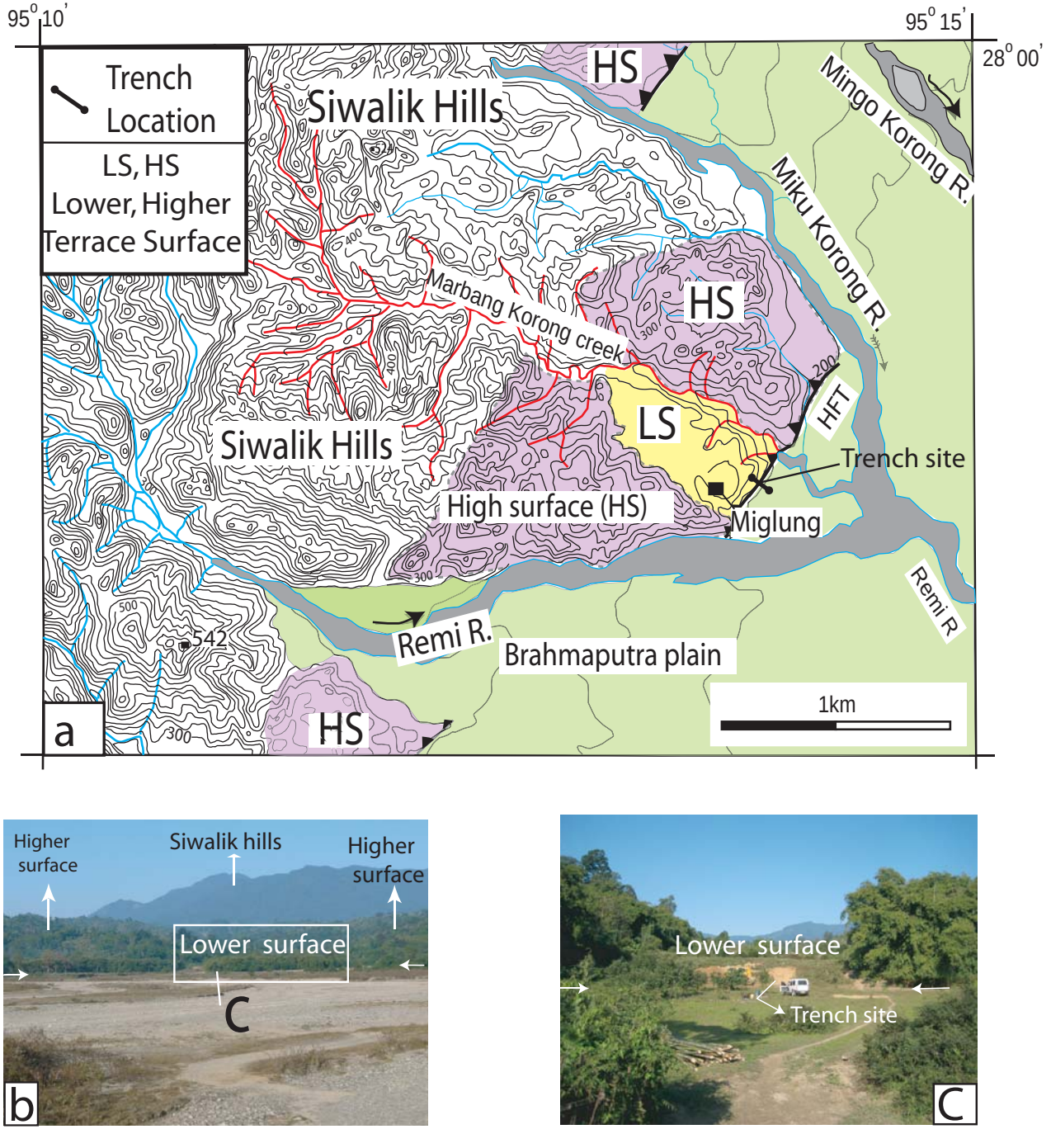

Figure 3

Figure4

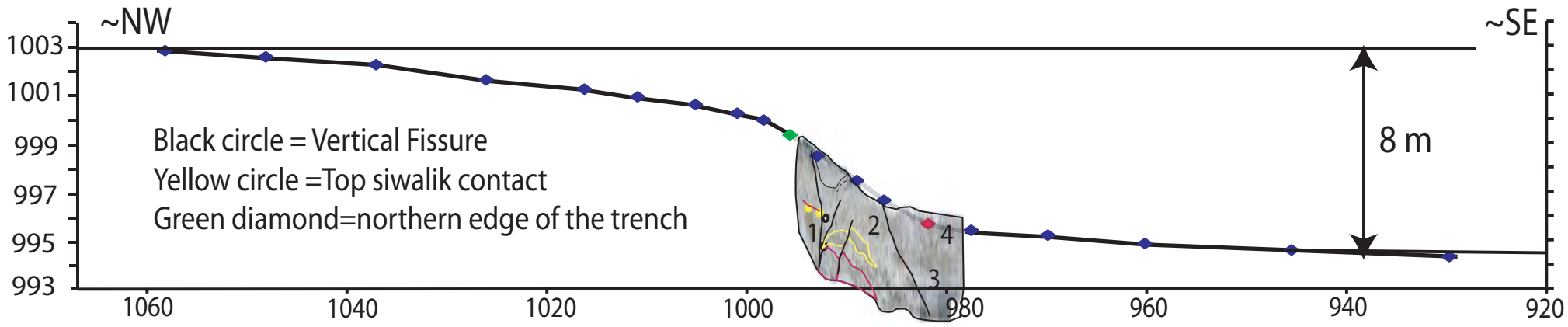

Figure 4

Figure5

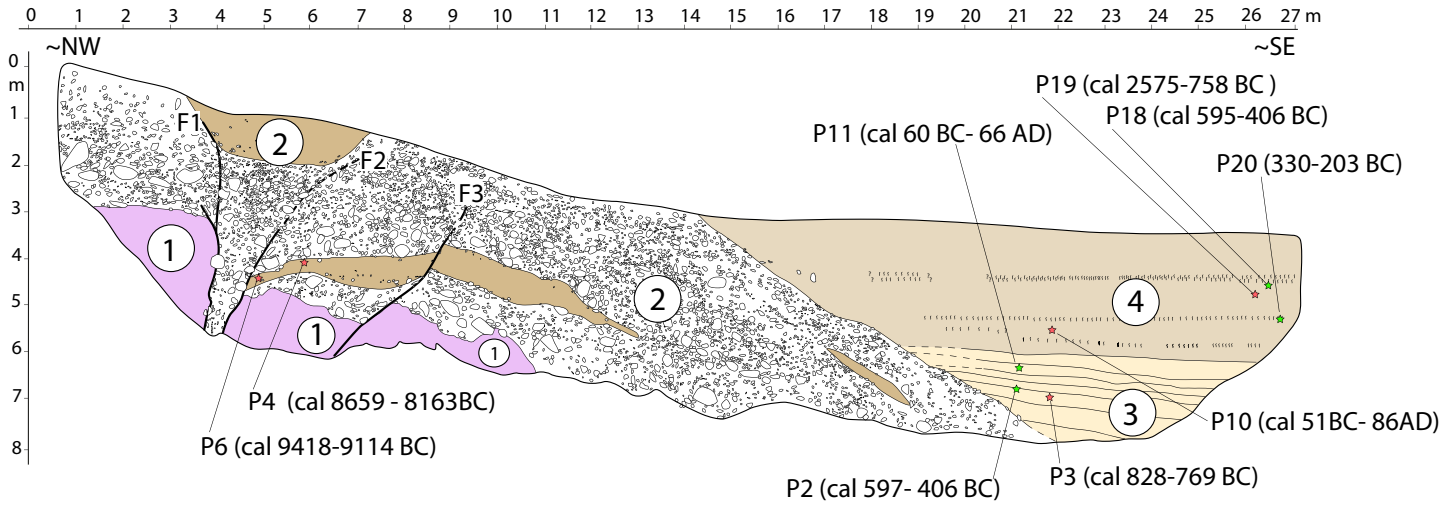

1 Bluish grey Siwalik sand stone, highly fractured

2 Sub rounded-sub angular pebbel to boulder, matrix supported. The size decreases towards top and becomes gravels with occas--sionaly large boulders. The unit is intercalated with dark brown lenses of silty sand.The unit shows nice dip panel that dip toward SE.

3 Clean white laminated tilted sand toward SE 10°. The unit is intercalated withsilty clay . Toward top it becomes fine sand brownish in color, hard massive, gravel with small burrows suggest the titled paleosurface shown as wavy line and is refered as Growth strata1.

4 Dark brown blocky horizontal fine silty sandy layer conformably sits on the unit 3. The horizontal wavy line is referred to soil horizon. The unit is refered as growth strata 2.

Figure 5

Figure6

Stage 1 = Penultimate earthquake
Post 8163 BC

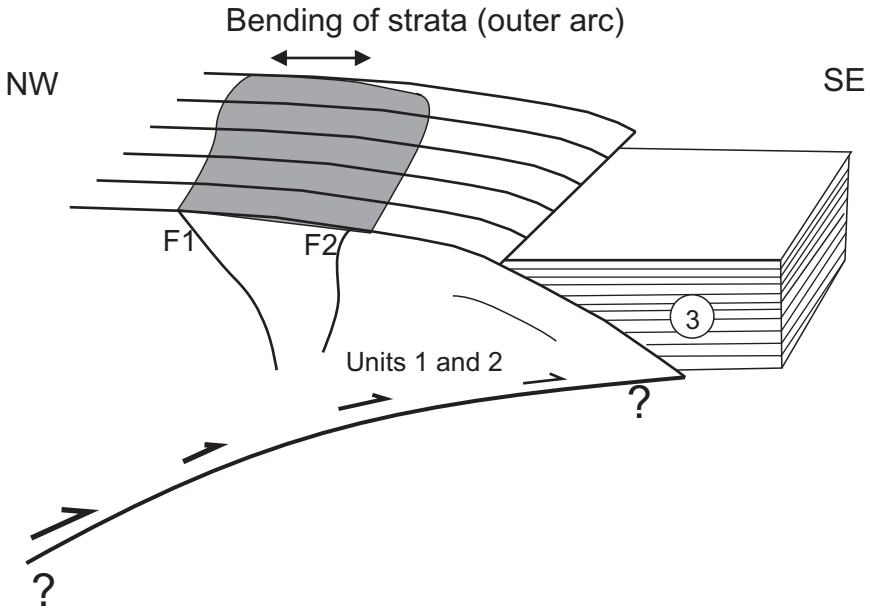

Stage 2 = Recent earthquake
Post 66 BC- 66AD

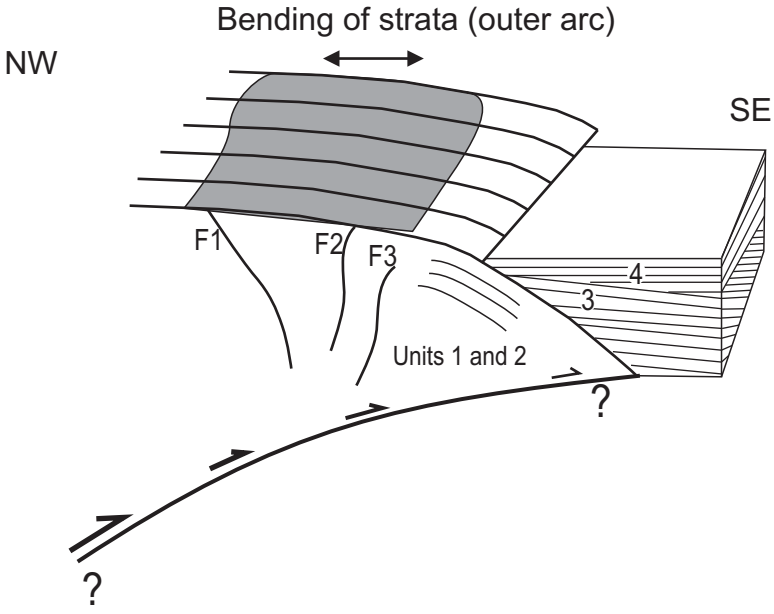

Figure 6

Supplemental Material Figure_1 Photomosaic

Click here to download Supplemental Material: 01Supplement_Figure_01.pdf